

# Photonic crystal devices for wavelength division multiplexing and slow photon generation

Wei Jiang<sup>1,2</sup>, Yongqiang Jiang<sup>1</sup>, Lanlan Gu<sup>1</sup>, Xiaonan Chen<sup>1</sup>, Yihong Chen<sup>2</sup>,  
Xiaolong Wang<sup>1</sup>, Weiping Bai<sup>1</sup>, and Ray T. Chen<sup>1</sup>

<sup>1</sup>Microelectronics Research Center and Department of Electrical and Computer Engineering,  
University of Texas at Austin, Austin, Texas 78758, USA

<sup>2</sup>Omega Optics, Austin, Texas 78758, USA

Photonic crystal based nanophotonic devices have been studied for various applications. One important type of devices are optical add-drop multiplexers (OADMs) that consist of photonic crystal cavities and waveguides. We show some novel device architectures and concepts to achieve better performance for such devices and discuss the non-vanishing backscattering issue. We fabricate high-quality photonic crystal waveguides on silicon-on-insulator substrates toward the ultimate goal of implementing the proposed OADM. Low optical loss, slow group velocity, and high dispersion are demonstrated in the fabricated waveguides, which is of interest to slow photon generation and optical delay line applications as well.

OCIS codes: 230.7370, 060.1810, 260.2030, 160.3130.

The explosive growth of Internet in the ending decade of last century has transformed almost all aspects of the society and our life. Accompanying the Internet marvel was an unprecedented demand of communication bandwidth, which was fortunately echoed by the fiber-optic communications technology, particularly the wavelength division multiplexing (WDM) technique. Meanwhile, the beginning of 21st century witnessed the pervasive influence of nanotechnology. In photonics, nano-scale structures, particularly photonic crystals<sup>[1-14]</sup>, hold the promise of achieving optical functions in a significantly reduced device size. Accompanying the size reduction is the exciting perspective of ultimate power reduction (e.g., thresholdless laser<sup>[1]</sup>), unprecedented dispersion enhancement<sup>[7,8]</sup>, and myriads of other benefits.

In this paper, we present our recent work on photonic crystal based optical devices, including optical add-drop multiplexers (OADMs) and optical true time delay lines.

Using photonic crystal based cavities and waveguides as building blocks, infinite opportunities in novel device configurations have emerged. One of such devices is a channel drop filter that selectively drops one specific wavelength from a broadband incoming light in a waveguide<sup>[4]</sup>. Such devices are usually called OADMs in WDM optical communications. The originally proposed structures have one or two pairs of cavities symmetrically placed between two parallel waveguides<sup>[4]</sup>. The working principle is that when the frequency of the light is close to the resonant frequencies of the cavities, light in one of the waveguides will be coupled to the cavity modes through evanescent tails in the waveguide cladding, and be further coupled into the other waveguide. By careful design, 100% light transfer to the other waveguide is shown possible.

In a recent letter, we have discussed the light drop processes in a more general situation, where  $n$  waveguides and  $n$  pairs of cavities are arranged in an  $n$ -fold symmetric structure<sup>[8]</sup>. Such a structure is characterized by a group  $C_{nv}$ . A structure for  $n=3$  is shown in Fig. 1. The analysis of these structure is considerably more difficult than that of the original structures, which correspond to a case of  $n=2$ . Consider the Hamiltonian of such a

system<sup>[8]</sup>

$$H = H_0 + V,$$

$$H_0 = \sum_{m=1}^n \sum_k \omega_k |mk\rangle \langle mk| + \sum_{m=1}^n \sum_c \omega_{mc} |mc\rangle \langle mc|,$$

$$V = \sum_{m,m'} \sum_{c,c'} (1 - \delta_{mm'} \delta_{cc'}) |mc\rangle \langle m'c'|$$

$$+ \sum_{m,m'} \sum_{k,c} [V_{mc,m'k} |mc\rangle \langle m'k| + V_{m'k,mc} |m'k\rangle \langle mc|],$$

where  $|mk\rangle$  is a propagating mode with wavevector  $k$  and frequency  $\omega_k$  in waveguide  $m$ , the mode  $|mc\rangle$  is a localized mode of the resonator pair next of waveguide mode  $m$ ,  $c = e$  and  $o$  for the even and odd modes, respectively;  $\omega_k$  is its frequency. The coefficients  $V_{mc,m'k}$  and  $V_{m'k,mc}$  represent the coupling between the corresponding modes.

It is desirable that through some simple transformation, the Hamiltonian  $H$  can be diagonalized. In the case  $n=2$ , this was done by transforming the modes of two adjacent single-mode cavities  $C_{i1}$  and  $C_{i2}$  ( $i=1,2$ ), into the even and odd modes (parity defined with respect to the

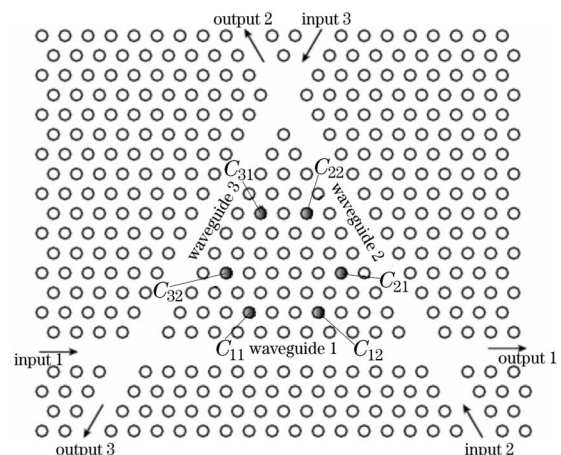


Fig. 1. Schematic drawing of an  $n=3$  symmetric OADM that consists of cavities and waveguides.  $C_{ij}$ : cavities.

mirror plane dividing the two cavities)<sup>[8]</sup>. Unfortunately, this is generally not possible for  $n > 2$ , even though the mirror symmetry exists in the system. Group theory indicates that for  $n > 2$ , the group  $C_{nv}$  is generally not an abelian group<sup>[15]</sup>. This means that the symmetry operations of the group  $C_{nv}$  do not commute with each other; therefore, irreducible representations of dimensions higher than unity appear. As a consequence, the even and odd modes are always coupled for each cavity pair  $C_{i1}$  and  $C_{i2}$ . Because of this, one has to work with partially diagonalized Hamiltonian.

This model is commonly solved through the Lippmann-Schwinger equation. Basically, the solving process is divided into two steps. 1) Find the condition for the backward scattering in all waveguides to vanish. 2) Find the condition for complete (or maximum) transfer to the desired drop waveguide. For an  $n$ -fold system, the complete light transfer to  $n-1$  drop waveguides occurs at  $n-1$  distinctive wavelengths. It is more convenient to use the symmetrized cavity modes, whose renormalized frequencies, intrinsic and extrinsic linewidths are denoted by  $\omega_{ac}$ ,  $\gamma_{ac}$  and  $\sigma_{ac}$ , respectively<sup>[8]</sup>. The extrinsic linewidths arise from the coupling to the waveguides.

The coupling of even and odd modes significantly complicated the process of finding the condition for zero backward scattering. Surprisingly, a condition can be found to simultaneously make background scattering vanish and diagonalize the self-energy, a key physical quantity in Lippmann-Schwinger theory<sup>[8]</sup>. In addition, we can show that slight deviation from this condition does not significantly degrade the system performance. For simplicity, the symmetrized mode index,  $\alpha$ , is omitted in the part. One can readily show that the normalized backscattering amplitude for a symmetrized mode<sup>[8]</sup> is given by

$$I_{\text{back}} \approx \gamma_1^2 |\Delta G(\omega)|^2,$$

where  $\gamma_1$  is a the intrinsic linewidth of one mode<sup>[8]</sup>, and the difference of the Green's functions between two cavity modes concerned is

$$|\Delta G(\omega)|^2 = \frac{\Delta\omega^2 + \Delta\Gamma^2}{[(\omega - \omega_1)^2 + \Gamma_1^2] \cdot [(\omega - \omega_2)^2 + \Gamma_2^2]},$$

where  $\omega_i$  and  $\Gamma_i$  are the renormalized mode frequency and linewidth<sup>[4]</sup>, and  $\Delta\omega = \omega_2 - \omega_1$ ,  $\Delta\Gamma = \Gamma_2 - \Gamma_1$ . When there is accidental degeneracy<sup>[4]</sup>, we have  $\Delta\omega = \Delta\Gamma = 0$ . Then the backscattering vanishes. Otherwise, it is straightforward to show that the maximum backscattering intensity is given by

$$(I_{\text{back}})_{\text{max}} \approx \frac{\gamma_1^2 (\Delta\omega^2 + \Delta\Gamma^2)}{\Gamma_1^2 \Gamma_2^2} \leq \frac{\Delta\omega^2 + \Delta\Gamma^2}{\Gamma_2^2}. \quad (1)$$

For example, a 10% deviation of  $\Gamma_i$  gives rise to about 1% (or -20dB) backscattering. Note that Eq. (1) is equally applicable to the  $n=2$  system.

In search for the complete drop condition, we found through some initial numerical calculations that a lossless system usually gives rise to a very poor filter performance. Dropping a narrow spectral band (e.g., 50 GHz) of light to a specific output port needs the collaboration of all other output ports. Unfortunately, the other

output ports always appear to extract a large amount of dropped light, regardless of our optimization efforts through varying the parameters of the system. Later, we rigorously proved that for a lossless system with  $n > 2$ , it is impossible to reduce the crosstalk in other un-intended waveguides (or the remnant light in the original waveguide) to a sufficiently low level over a finite band of spectrum. However, in a lossy system, with ingenious design, a complete transfer with desirable filter spectral profile is possible. This is one of the most intriguing discoveries of our work. An example solved by our theory is shown in Fig. 2. It is evident from Fig. 2(d) that the deliberately introduced loss suppresses the remnant light intensity near the dropped frequency band in the input waveguide, which is advantageous to the system.

In early experimental studies of such photonic crystal based OADM, the vertical leaking of light resulted in surface-normal output of light<sup>[6]</sup>. Recently, exciting progress was seen to realize such OADM in a fully integrated fashion<sup>[7]</sup>. In light of these discoveries, we conducted experimental work on two-dimensional (2D) photonic crystals with the ultimate goal of implementing the photonic crystal OADM system discussed above as well as other nanophotonic devices.

Photonic crystal slabs are 2D Photonic crystal structures located within slab waveguides. In Photonic crystal slabs, light is confined by a combination of in-plane photonic bandgap (PBG) confinement and vertical index guiding. One simple way to utilize the PBG effect is to introduce functional defects into Photonic crystals, which is analogous to doping intentional defects in electronic crystals to introduce defect bands. Line defects can work as strongly confined waveguides<sup>[10]</sup>. Due to all these unique properties and easy fabrication techniques, 2D Photonic crystal slab line defect waveguides have been extensively studied<sup>[10-14]</sup>. One of the most interesting and exciting properties is the high group velocity dispersion (GVD) and slow photon effect near transmission band edge. Notomi *et al.* first demonstrated high dispersion and slow photon effect using silicon photonic crystal

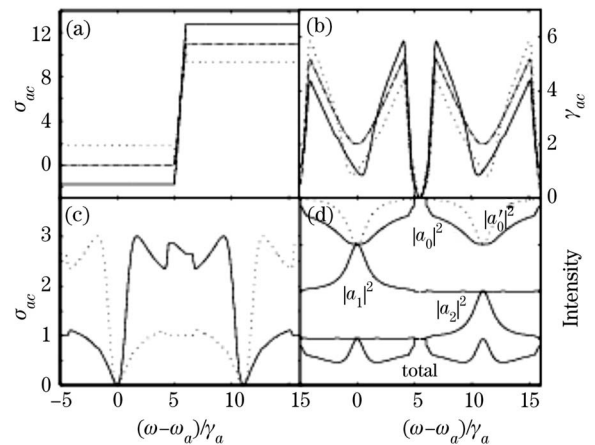


Fig. 2. (a)-(c) The solved cavity parameters  $\omega_{ac}$ ,  $\gamma_{ac}$ , and  $\sigma_{ac}$ . Dashdot, solid, and dotted lines correspond to  $\alpha=0, 1, 2$ , respectively. (d) Reconstructed spectra are shown in (d) on a linear scale, where  $|a_0|^2$  (dotted line) is a reference lossless spectrum. Each intensity reaches maximum 1 and minimum 0, except the total intensity, whose minimum is greater than zero.

waveguides<sup>[10]</sup>. Several other groups also demonstrated this effect in both line defects and coupled-cavity photonic crystal waveguides<sup>[12,13]</sup>. While slowing down photon or stopping light itself is a topic of great interest to the scientific community, there are many interesting applications of slow photon generation. For example, slowed photons are expected to interact stronger with materials, resulting in enhanced nonlinear optical effects in certain materials<sup>[14]</sup>. With such enhancement, short interaction lengths are needed to demultiplex, modulate, switch, deflect, or wavelength-convert light. In this part, we will present design and fabrication of line defect photonic crystal waveguides in 2D slabs for slow photon generation.

The photonic crystal waveguides are designed by three-dimensional (3D) full-vectorial plane wave expansion (PWE) method<sup>[10]</sup>. Proper parameters are chosen such that the guided modes of the waveguides are around the telecommunication wavelength  $1.55 \mu\text{m}$ . We fabricated the designed Photonic crystal waveguides on a silicon-on-insulator (SOI) wafer. Photonic crystal structures are patterned by electron beam lithography. After developing the resist, the patterns are transferred to a thin oxide mask layer by reactive ion etching, followed by the resist removal. Finally the patterns are transferred to the silicon layer with the oxide layer as the hard mask through another dry etching process. Devices with lattice constant  $a = 400 \text{ nm}$ , air hole diameter  $d = 210 \text{ nm}$ , and slab thickness  $t = 215 \text{ nm}$  are fabricated. Post-etching oxidation at  $850^\circ\text{C}$  is implemented. The post-etching oxidation forms an additional thin oxide layer, making the side-wall of air-holes significantly smoother than the original surface after dry etching. Extensive experimentation with various processes has been conducted to determine the optimized process parameters. We have introduced a proper pre-offset of the hole size in e-beam pattern design so that the hole size can be controlled with an accuracy of 5%. A number of scanning electron microscopic (SEM) micrographs are shown in Fig. 3, which demonstrates the high quality of the silicon nano-structures fabricated through our optimized processes.

The optical transmission and dispersion of photonic crystal waveguide modes are characterized. Two lensed fibers are manipulated by two automated 5-axis stages, which are controlled by a computer to precisely align the fibers with the silicon waveguides. Propagation loss below  $6 \text{ dB/mm}$  is measured. The group index  $n_g = c/v_g$  can be calculated directly from the varying Fabry-Perot

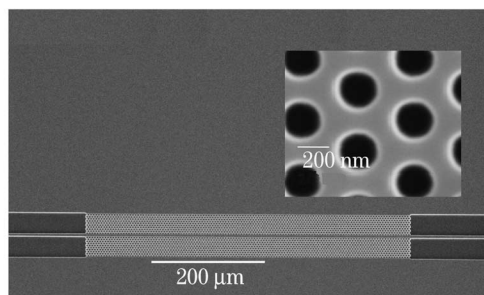


Fig. 3. SEM micrographs of the nano-structures of silicon photonic crystal waveguides. Details of this waveguide are magnified.

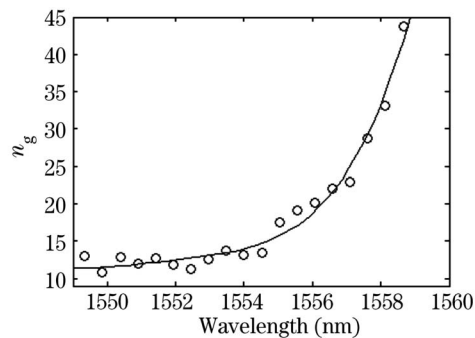


Fig. 4. Group index  $n_g$  for a photonic crystal waveguide. Circles represent  $n_g$  obtained from the experimental spectrum via short-time Fourier transform; the line is added to indicate the trend. Pronounced increase of  $n_g$  is evident, as anticipated from the theory.

oscillation period of transmission spectrum<sup>[11]</sup>. Such calculations may be subject to uncertainty and fluctuation due to spectrum noise and wavelength digitization. Similar problems occur in analyzing signals such digitized human voice, and the countermeasures are well established. Here we introduced a simple short-time Fourier transform algorithm<sup>[16]</sup>, which recovers the wavelength-dependent oscillation period of experimental transmission spectra and compute  $n_g$  with low fluctuation. Figure 4 attests the high  $n_g$  values as anticipated. The GVD is also calculated to be  $50 \text{ ps}/(\text{nm}\cdot\text{mm})$  at  $1558 \text{ nm}$ . The dispersion increases by  $10^7$  times in comparison with standard telecom LEAF fibers that have a dispersion parameter of  $3 \text{ ps}/(\text{nm}\cdot\text{km})$ . In certain optical-delay-line based devices<sup>[17]</sup>, an extremely low group velocity or a high GVD could help to significantly shorten the device length<sup>[18]</sup>. Note that slow group velocity can also be achieved in photonic crystals without introducing line defects<sup>[19]</sup>.

In summary, OADMs are investigated based on novel photonic crystal structures. Suppression of remnant light in the dropped frequency bands of the pass-through port is demonstrated, and backscattering is found to be relatively insensitive to the deviation from the accidental degeneracy of cavity modes. Photonic crystal waveguides are experimentally studied toward the ultimate goal of implementing the proposed OADM. Low optical loss, slow group velocity, and high dispersion are demonstrated.

This work was supported by the National Science Foundation and Air Force Office of Scientific Research of USA.

## References

1. E. Yablonovitch, Phys. Rev. Lett. **58**, 2059 (1987).
2. S. John, Phys. Rev. Lett. **58**, 2486 (1987).
3. J. D. Joannopoulos, R. D. Meade, and J. Winn, *Photonic Crystals* (Princeton University Press, Princeton, 1995).
4. S. Fan, P. R. Villeneuve, J. D. Joannopoulos, and H. A. Haus, Phys. Rev. Lett. **80**, 960 (1998).
5. Y. Xu, Y. Li, R. K. Lee, and A. Yariv, Phys. Rev. E **62**, 7389 (2000).
6. Y. Akahane, T. Asano, B. S. Song, and S. Noda, Nature **425**, 944 (2003).

7. Y. Akahane, T. Asano, B. S. Song, Y. Takana, and S. Noda, *Opt. Express* **13**, 2512 (2005).
8. W. Jiang and R. T. Chen, *Phys. Rev. Lett.* **91**, 213901 (2003).
9. W. Jiang, J. Zou, L. Wu, Y. Chen, C. Tian, B. Howley, X. Lu, and R. T. Chen, *Proc. SPIE* **5360**, 190 (2004).
10. S. G. Johnson, S. Fan, P. R. Vileneuve, J. D. Joannopoulos, and L. A. Kolodziejski, *Phys. Rev. B* **60**, 5751 (1999).
11. M. Notomi, K. Yamada, A. Shinya, J. Takahashi, and I. Yokohama, *Phys. Rev. Lett.* **87**, 253902 (2001).
12. T. J. Karle, Y. J. Chai, C. N. Morgan, I. H. White, and T. F. Krauss, *J. Lightwave Technol.* **22**, 514 (2004).
13. D. Mori and T. Baba, *App. Phys. Lett.* **85**, 1101 (2004).
14. M. Soljacic and J. D. Joannopoulos, *Nature Materials* **2**, 211 (2004).
15. J. Q. Chen, *Group Representation Theory for Physicists* (World Scientific, Singapore, 1989).
16. A. V. Oppenheim, (ed.) *Applications of Digital Signal Processing* (Prentice-Hall, Englewood Cliffs, 1978).
17. Y. H. Chen, K. Wu, F. Zhao, and R. T. Chen, *Proceedings of the 2004 IEEE Antennas and Propagation Society Symposium* **14**, 4324 (2004).
18. K. Hosomi and T. Katsuyama, *IEEE J. Quantum Electron.* **38**, 825 (2002).
19. W. Jiang, R. T. Chen, and X. Lu, *Phys. Rev. B* **71**, 245115 (2005).